Eukaryotic membrane tethers revisited using magnetic tweezers

2007 Phys. Biol. 4 67

(http://iopscience.iop.org/1478-3975/4/2/001)

Phys. Biol. **4** (2007) 67–78 doi:10.1088/1478-3975/4/2/001

Eukaryotic membrane tethers revisited using magnetic tweezers

Basarab G Hosu[1], Mingzhai Sun[2], Françoise Marga[2], Michel Grandbois[3] and Gabor Forgacs[1,2]

[1] Department of Biological Sciences, University of Missouri, Columbia, MO 65211, USA
[2] Department of Physics, University of Missouri, Columbia, MO 65211, USA
[3] Département de Pharmacologie, Université de Sherbrooke, Sherbrooke, QC, J1H 5N4, Canada

Received 16 December 2006
Accepted for publication 26 March 2007
Published 19 April 2007
Online at stacks.iop.org/PhysBio/4/67

Abstract

Membrane nanotubes, under physiological conditions, typically form *en masse*. We employed magnetic tweezers (MTW) to extract tethers from human brain tumor cells and compared their biophysical properties with tethers extracted after disruption of the cytoskeleton and from a strongly differing cell type, Chinese hamster ovary cells. In this method, the constant force produced with the MTW is transduced to cells through super-paramagnetic beads attached to the cell membrane. Multiple sudden jumps in bead velocity were manifest in the recorded bead displacement–time profiles. These discrete events were interpreted as successive ruptures of individual tethers. Observation with scanning electron microscopy supported the simultaneous existence of multiple tethers. The physical characteristics, in particular, the number and viscoelastic properties of the extracted tethers were determined from the analytic fit to bead trajectories, provided by a standard model of viscoelasticity. Comparison of tethers formed with MTW and atomic force microscopy (AFM), a technique where the cantilever–force transducer is moved at constant velocity, revealed significant differences in the two methods of tether formation. Our findings imply that extreme care must be used to interpret the outcome of tether pulling experiments performed with single molecular techniques (MTW, AFM, optical tweezers, etc). First, the different methods may be testing distinct membrane structures with distinct properties. Second, as soon as a true cell membrane (as opposed to that of a vesicle) can attach to a substrate, upon pulling on it, multiple nonspecific membrane tethers may be generated. Therefore, under physiological conditions, distinguishing between tethers formed through specific and nonspecific interactions is highly nontrivial if at all possible.

1. Introduction

Membrane nanotubes or tethers are protrusions from the surface of lipid bilayers and are involved in numerous cellular processes. They form during leukocyte attachment to and rolling along the endothelial wall [1–3] or as precursors to extravasation of cancer cells in the course of metastatic spreading [4]. They provide intercellular [5–8] and intracellular [6–10] communication channels. They participate in adhesion [11], migration and signaling [12]. Membrane tethers can form through active processes governed by actin [5] and microtubule polymerization [6] or by the activity of molecular motors [13–15]. In leukocyte rolling they are passively pulled from preexisting membrane structures (i.e. microvilli) through specific receptor–ligand bonds upon contact with endothelial cells or platelets [1].

Tether formation requires changes in the shape of the underlying membrane, and thus is strongly dependent on the membrane's mechanical characteristics. For phospholipid vesicles, theory [16–19] provides an accurate, experimentally tested account of tether formation in terms of membrane tension and bending rigidity [15, 20, 21]. The situation with living cells is more complicated [22, 23]. The eukaryotic plasma membrane is sandwiched between and molecularly coupled to two macromolecular networks: the intracellular cortical cytoskeleton and the extracellular glycocalyx. In addition, specialized domains (e.g. rafts) and the myriad of embedded molecular entities, make the plasma membrane

highly heterogeneous. As a consequence, tethers sprouting at distinct locations along the cell surface (e.g. apical and basolateral surface of epithelial cells [24], microvilli [25], blebs [24], leading and trailing edge of migrating cells [11]) or from distinct intracellular membranes (e.g. Golgi versus endoplasmic reticulum [10]) could have differing material properties [12].

Membrane nanotubes have been extracted by special force transducers (optical tweezers [26–29], magnetic tweezers [30], aspirating micropipettes [31–33]) from vesicles or a wide range of cell types (red blood cells [34], neutrophils [33, 35], neurons [36], fibroblasts [37, 38], as well as epithelial [24] and endothelial cells [31]). In such experiments tethers form passively and no microfilaments are present inside the elongating nanotubes [27]. With a few exceptions mechanical extraction studies have concentrated on single tethers pulled from particular locations [12]. Double tethers have been extracted from living cells by Xu and Shao [39] and from synthetic vesicles by Cuvelier *et al* [20].

Recent results suggest that multiple tether formation may be a control mechanism in physiological processes [2]. In particular, it was shown that the number of tethers extracted from neutrophils in the course of their rolling increases with rising endothelial wall shear stress. The multiplicity (and thus the varying strength) of these transient attachments serves as a regulator of the cells' rolling under changing hydrodynamic conditions [1, 2]. Entire networks of membrane nanotubes have been observed in the interior of eukaryotic cells [7, 8] with likely role in the physical contact between intracellular membrane bound organelles. These findings suggest that cells can form and maintain multiple tethers and use them in various physiological processes.

Sun and collaborators [40] recently have used atomic force microscopy (AFM) to extract tethers, formed through nonspecific interactions from a number of cell types. They provided suggestive evidence for the existence of multiple, simultaneously forming tethers. These were identified by abrupt drops in force–cantilever elongation profiles indicating the sequential detachment of individual tethers from the cantilever in the course of its retraction. The main objective of [40] was to show that multiple nonspecific tether formation is a ubiquitous phenomenon in eukaryotic cells that is readily observed when a cell is allowed to adhere to a surface. For this, both qualitative and quantitative evidence was provided. In particular, the average force required to form a single tether was found to be ∼30 pN (at 3 μm s^{-1} cantilever retraction speed), irrespective of the (three) cell types used. While this value was also independent of the chemical nature of the attachment to the cantilever it strongly decreased when the cell's actin cytoskeleton was partially disrupted or its hyaluronan glycocalyx removed. The findings in [40] also indicated that if multiple tethers indeed can be extracted simultaneously, due to strong inhomogeneities in true cell membranes, contrary to the situation in lipid vesicles [19, 20], they are pinned and do not interact.

The evidence in [40] for the existence of simultaneously sprouting tethers was circumstantial. Furthermore, due to the way tethers are extracted with AFM, it was not possible to determine, whether they originated from preexisting structures (e.g. microvilli) or formed *de novo*. The objective of the present work was to further investigate the complexity of eukaryotic membrane tethers in living cells by addressing primarily the above uncertainties. Thus we first used scanning electron microscopy (SEM) to visualize the putative multiple membrane nanotubes. Second, to explore which part of the plasma membrane may give rise to these tethers we sought for a more gentle method of generating them. As presented below, both objectives were possible to reach by employing magnetic tweezers (MTW). The two techniques, AFM (for reviews see [41, 42]) and MTW (for a review see [43]) have overlapping but also complementary capabilities. The AFM draws tethers at constant velocity (AFM tethers in what follows), whereas the MTW does it at constant force (MTW tethers in what follows). Both devices can exert forces from piconewtons to nanonewtons and thus provide the opportunity to monitor the formation of individual or multiple tethers and study their biophysical properties. Comparison of these properties across AFM and MTW tethers, as will be discussed, provides useful information, which cannot be deduced solely by using only one of these methods.

2. Materials and methods

2.1. Cell cultures and treatment

Two cell types have been used in the present study. HB, a human brain tumor cell line was kindly provided by B Hegedüs (National Institute of Neurosurgery in Budapest, Hungary, [44]), whereas Chinese hamster ovary (CHO) cells were purchased from the American Type Culture Collection (ATCC, Manassas, VA). Cells were grown at 37 °C in 5% CO_2 on 75 cm^2 TC dishes in DMEM (Invitrogen Corp., Carlsbad, CA) containing 10% FBS (US Bio-Technologies, Pottstown, PA), 10 μg ml^{-1} penicillin, streptomycin, gentamicin and kanamycin sulphate (Invitrogen Corp., Carlsbad, CA). Media were supplemented with 1 μg ml^{-1} Fungizone (Invitrogen Corp., Carlsbad, CA) for HB culture. Twenty four hours before an experiment, cells were plated on glass coverslips, placed in 35 mm plastic Petri dishes and allowed to reach 30–50% confluence in the conditions described above. Coverslips were then washed twice with PBS (Invitrogen Corp., Carlsbad, CA), transferred to CO_2 independent medium, containing 2% FBS and supplemented with antibiotics (as above). In cytoskeletal disruption experiments, the cells were kept in CO_2 independent medium supplemented with latrunculin A (Sigma, St. Louis, MO), a specific actin polymerization inhibitor (45–47) at 1.0 μM concentration for 30 min before the measurement.

2.2. Tether extraction with magnetic tweezers

Thirty minutes before an experiment a suspension of 5 μm super-paramagnetic beads (2 × 10^5 beads ml^{-1} in PBS; Dynabeads M-500, Dynal ASA, Oslo, Norway) was prepared. (Coefficient of bead size and shape variation <3%, by the manufacturer's specification.) The beads are composed of a magnetic core embedded in polystyrene and their surface provides reactive groups for ligands, containing primary

amino- or sulfhydryl groups. The bead solution was homogenized, for 5 min, with a Model 250 Brenson sonifier (Brenson, Danbury, CT). Immediately prior to an experiment, a cell-plated triangular coverslip (fabricated by cutting 18 mm square coverslips (Corning Inc., Corning, NY)) was transferred into a removable sample holder, which fits between the two poles of the MTW, mounted on the stage of an Olympus IX70 inverted microscope (as described in [43]), Cells were first covered with about 200 μl of CO_2 independent medium to which subsequently 10 μl of the bead suspension was added. Beads, having density of 1.5 g cm^{-3}, slowly descended on the coverslip and those that landed on cells, adhered to them. Beads typically were in contact with cells for 1 min prior to the application of the magnetic force (for details on the magnetic tweezers, in particular its calibration, see [43]). Experiments were conducted at room temperature. To identify a bead capable of pulling a tether, a few short magnetic force pulses (1 Hz, 50% duty cycle) were applied continuously with simultaneous optical scanning of the sample. To minimize the probability of rupturing the tethers during this search phase, the magnitude of these force pulses was small, typically 1–20 pN, corresponding to the minimum force which could visibly reversibly displace a bead attached to the membrane. Once a tether-pulling bead was identified, a long (typically 20 s) pulse, typically at a higher force (set by the current through the coils) was applied to it. The total contact time between the bead and the cell surface, prior to tether extraction was about 60 s. Under such conditions, in any one particular experiment several tether-pulling beads could be located for both cell types. Since bead position could not be controlled (beads could land anywhere on the coverslip), the applied forces ranged from 15 to 1500 pN. Owing to the design of our MTW, extraction of tethers by a particular bead took place under constant force along a well-defined direction (for details see [43]). Bead trajectories were acquired in bright field with a CoolSNAPfx digital video camera (Photometrics, Tucson, AZ), using a 20× objective. Displacement–time curves were recorded and analyzed with sub-pixel precision (∼20 nm) using Image Pro Express (IPE; Media Cybernetics, San Diego, CA) and in-house developed particle tracking software. The software is composed of a set of Labview (National Instruments Corp., Austin, TX) programs, which, in brief, perform the following tasks. During the recording of bead trajectory (by IPE), the program determines the exposure time of each frame, the time interval between frames and the time interval between the beginning of the magnetic pulse and the subsequent camera frame (parameters needed for accurate tracking). These data are generated by digital signals provided by the camera and the magnetic tweezers and acquired through a digital NI I/O board. After video acquisition, the program converts the IPE-generated sequence files into three-dimensional pixel-map Labview arrays, with each element of the array representing the brightness of the corresponding pixels. Finally, the program compares these arrays for subsequent frames. This procedure provides the trajectory of the bead on the basis of changes in pixel brightness. Displacements smaller than a pixel translate in changes of pixel brightness at the edge of the bead. All hardware (MTW, microscope stage and the video camera) was controlled and integrated using Labview.

2.3. Visualization of cell surface and tethers

We used SEM to observe the surface of HB and CHO cells at high magnification to explore the possible sources of membrane tethers in these cells. In conjunction with MTW, SEM was also used to visualize individual and multiple tethers. For this, cells were cultured (as described above) on 12 mm round coverslips instead of the triangular-shaped ones used in the other experiments. These were placed into a modified sample holder (to accommodate the round coverslips) beneath the plane of the magnetic poles of the MTW, thus creating a force on the magnetic beads oriented slightly upward (away from the coverslip). While applying a long continuous pulse, the sample was slowly raised above the plane of the poles. (Unlike a triangular coverslip, a round coverslip does not fit well in between the poles. Therefore during the SEM experiments beads were further from the poles and thus the magnetic force acting on them was smaller than in the regular tether pulling case described above.) By this maneuver, the direction of the force was gradually changed from upward to downward (toward the coverslip). As a result, the beads eventually came in contact with the glass surface and halted. Thus the tethers extracted by the beads extended between two immobilized objects (the bead and the cell). Once this point was reached, the sample was fixed (while still applying the magnetic force) by adding 250 μl of 2.5% glutaraldehyde (Electron Microscopy Sciences, Hatfield, PA) in PBS solution. Ten minutes after adding the fixative, the magnetic field was turned off and the coverslips transferred and kept in a Petri dish (containing the same fixative) for an additional 80 min. The fixative was then removed by three rinses in PBS, the coverslips transferred into a holder and plunged for 30 min in an increasing concentration series of ethanol as follows: 10%, 25%, 50%, 75%, 95%. Finally, the holder was kept in 100% ethanol overnight. The dehydration of the sample was completed in a Samdri-PVT-3B (Tousimis, Rockville, MD) critical point drier by exchanging ethanol to liquid CO_2 and sublimating the latter. Subsequently, the coverslips were maintained on stub using carbon adhesive tabs; in each case three copper strips were circularly arranged to provide maximal electrical conductivity. The samples were sputter coated with platinum at 5 mA for 45 s before examination with a Hitachi S4700 cold-cathode field-emission scanning electron microscope at an accelerating voltage of 5 kV. Membrane tethers were also observed in bright field optical microscopy.

3. Results and discussion

3.1. Possible sources of membrane tethers in HB and CHO cells

SEM images of the cell surface, as shown in figure 1, indicate that both cell types have numerous microvilli along their plasma membrane. These images also suggest that microvilli are of sub-micron length (in good agreement with the findings in [25]). It has been demonstrated that under a pulling force

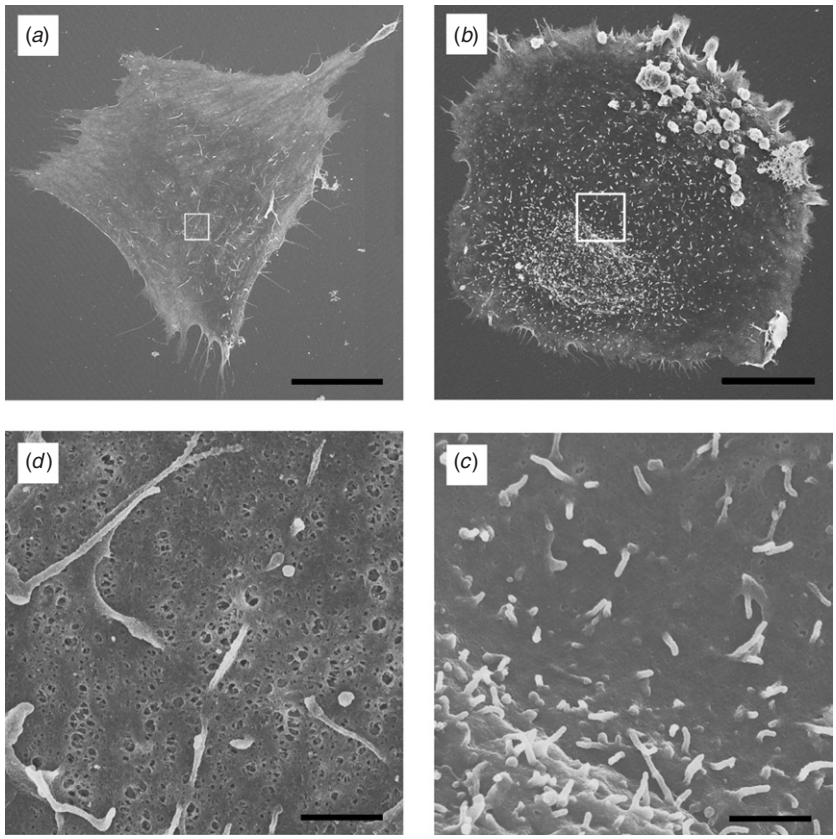

Figure 1. (*a*), (*b*) SEM micrographs of a HB (*a*) and CHO (*b*) cell surface. (*c*), (*d*) The surface morphology within the boxed areas of the two cell types HB (*c*), CHO (*d*). Scale bars: 20 μm in (*a*) and 10 μm in (*b*); 1 μm in (*c*), (*d*).

a microvillus can be extended or a tether can be formed from it [25]. Since a 5 μm magnetic bead or a cantilever can simultaneously attach to many microvilli, in principle it can easily pull multiple tethers. At the same time the flat portions of the cell surface are also potential sources of membrane nanotubes, immediately raising the question how these two types of tethers compare.

3.2. Visualization of multiple tethers

Images in figure 2 offer a wealth of information. First, they evidence that in the MTW experiments indeed multiple tethers can be simultaneously extracted. Multiple tubular membrane structures connect the beads to the plasma membrane (panel (*b*)). Second, comparing the bright field image with the SEM images suggests that the structures in figure 2(*a*) could actually represent bundles of nanotubes (individual structures within one bundle could not be resolved by optical microscopy). Third, the SEM images provide a rough estimate for the radius of the tubes: 72 ± 17 and 65 ± 17 nm (mean$\pm$standard deviation) for CHO (21 measurements along 7 tethers) and HB (37 measurements along 10 tethers) cells, respectively.

3.3. Manifestation of multiple tethers in MTW and AFM experiments

Tether extraction with MTW takes place under constant force applied to a magnetic bead whose position is recorded as function of time (figure 3, left panels). As can be seen in figure the slope of the magnetic bead's trajectory changes abruptly at discrete points, which means that at these points the bead's velocity jumps. Figure 2 provides visual evidence for the simultaneous existence of multiple tethers. Comparison of figures 2 and 3 thus strongly suggests that the jumps correspond to the detachment or rupture of individual tethers. Similar discrete events have been observed in the velocity of leukocytes rolling on selectin coated surfaces and also interpreted in terms of multiple bonding between the cell and the substrate [1]. Since the magnetic force exerted on the bead is constant along its entire trajectory, when one of the tethers ruptures, the bead accelerates, and the remaining tethers experience a larger force (i.e. larger velocity). Once the magnetic force is turned of the bead eventually returns to its original location and no rupture events are detected (parts of this recovery can be seen in figure 3). An example of the typical variation in velocity along a bead trajectory is shown in the context of figure 5 below. (Note that the magnitude of the jump in velocity at rupture depends on where the rupture, a stochastic event, takes place. Therefore velocity values at subsequent ruptures need not exhibit monotonic increase, as is the case in figure 5.) For comparison, in the right panels of figure 3 we reproduce force–cantilever elongation profiles obtained with AFM, which shows that the presence of simultaneously existing multiple tethers and their sequential rupture in this technique are manifest as sharp drops of similar magnitude in the measured force value (compare with figure 3 in [40]).

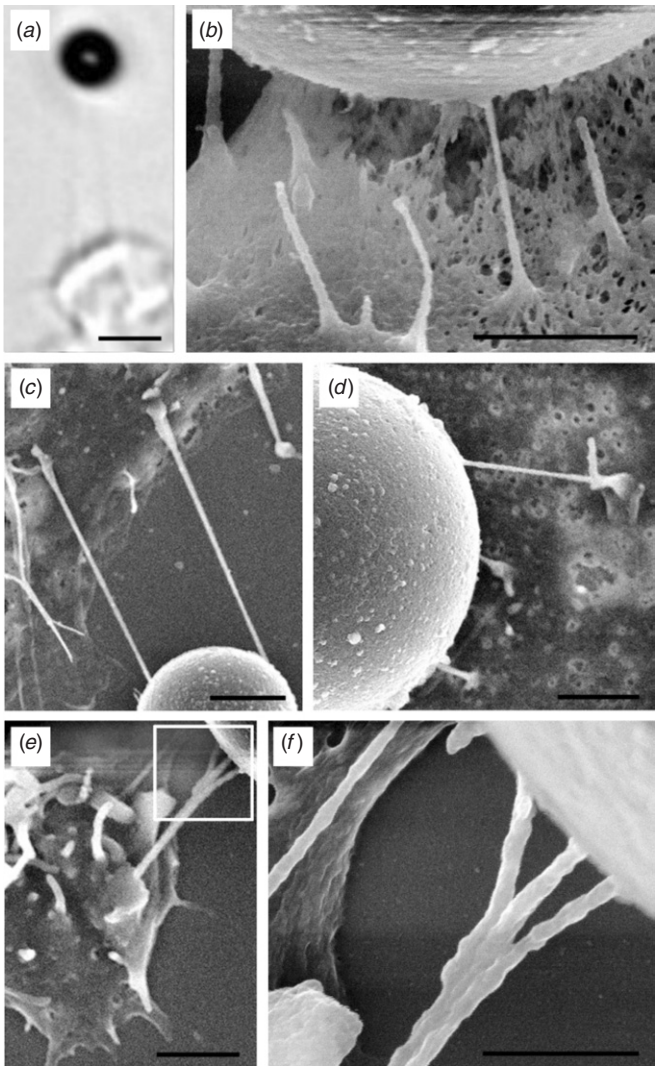

Figure 2. (*a*) Multiple tethers (faint shadows) visualized by bright field optical microscopy. Two tether-like structures are seen emanating from a HB cell (bottom). (*b*)–(*f*) Representative SEM micrographs of membrane tethers pulled from cells of different type. Multiple tethers are formed between the 5 μm bead and the membrane of CHO cells (*b*) and HB cells (*c*)–(*f*). Panels (*b*)–(*e*) suggest that these tethers originate from pre-existing structures. Panels (*e*) and (*f*) are suggestive of rupture events which (as well as the fusion of the three tethers) may be the consequence of sample preparation for SEM. Panel (*f*) is the enlargement of the boxed area in (*e*). Scale bars: 5 μm in (*a*); 1 μm in (*b*), (*d*), (*e*); 2 μm in (*c*); 500 nm in (*f*).

The drops separate plateau regions where the force acting on the cantilever is constant. The force drop is the tether force, needed to pull a single (in particular the last) tether. A force peak (referred to below as 'initiation force') is typically present at the beginning of the pulling.

3.4. Quantitative analysis of the MTW results

A segment of the bead trajectory in figure 3 (representing a collection of tethers) between two subsequent rupture events, in particular after the ith one ($i = 0, 1, \ldots, N-1$; N—total number of extracted tethers), $x_i(t)$ was fit with a simple exponential $x_i(t) = A_i\left(1 - \mathrm{e}^{-(t-t_i^0)/\tau_i}\right)$ (lines over data points). The quantity t_i^0 denotes the time where the exponential function used for the fit would cross the horizontal axis. To relate the fitting parameters to physical quantities, we constructed a minimal model of multiple tether formation by MTW (figure 4): we represented each of the N initial tethers with an identical Voight body (a dashpot, characterized by a friction constant μ, in parallel with a spring, with spring constant k), a widely used element in phenomenological models of viscoelasticity [48]. The friction between the magnetic bead and the cell culture medium is represented by μ_m ($\mu_m = 6\pi\eta R \approx 0.05$ pNs μm^{-1} with $R = 2.5$ μm the radius of the magnetic bead, and $\eta \approx 10^{-3}$ Pa s the viscosity of the culture medium, approximately that of water). This simplification is equivalent to assuming that the different tethers do not interact and are composed of the same material. This is consistent with the earlier result of the AFM study, which suggests that the tether force for a given velocity is the same for each tether (extracted from a given cell type [40]). The solution of this model provides the same exponential form as above and identifies the constants in that expression in terms of the model parameters: $A_i = F/[k(N-i)]$ and $\tau_i = [\mu + \mu_m/(N-i)]/k$. Here A_i and τ_i correspond to the bead trajectory after i ($=0, 1, \ldots, N-1$) tethers have ruptured, and F is the constant force exerted by the MTW on the magnetic bead. (Note that when the bead is pulling $N-i$ tethers the effective friction hindering its movement is $(N-i)\mu + \mu_m$. Also note that μ_m is not that different from the values listed in table 1 for the tethers.)

The experimental results allow estimating all the model parameters, in particular the total number of tethers, N, extracted in each experiment. (Employing the bead trajectories to count N is useful only in those (few) pulling experiments in which by the end of the magnetic pulse all tethers have ruptured; see figure 5.) We consider A_i as a continuous function of its index and fit the experimental results for this quantity to a hyperbola, as given by the model. The outcome of this procedure, shown in figure 5, provides values for k, N and μ (for the latter through the experimentally determined $\tau_i = [\mu + \mu_m/(N-i)]/k$) listed in table 1. (Not all pulling curves showed ruptures. In fact for the above analysis of N only curves with at least three ruptures were used.)

3.5. Viscoelastic properties of AFM tethers

To compare the physical characteristics of MTW and AFM tethers we performed AFM tether pulling experiments at variable cantilever retraction speeds (measurements in [40] were performed only at 3 μm s^{-1}). (For details on how AFM tether pulling experiments are performed and evaluated, see [40].)

The results in figure 6 indicate that for the pulling velocities used in the present work (3, 9, 15 and 21 μm s^{-1}) the relationship $F = F^0 + \mu v$ is fulfilled [30, 31, 39] and non-Newtonian shear-thinning behavior is not detected [49]. Here F, F^0, v and μ are respectively the tether force, the threshold value of F, the retraction speed and the friction constant, the latter being related to the effective surface viscosity η_s,

Table 1. Summary of the quantitative results obtained in this study.

Cell type (treatment)	μ (pNs μm^{-1}) MTW (Mean ± SEM)	μ (pNs μm^{-1}) AFM (Mean ± SD)	k (pN μm^{-1}) MTW (Mean ± SEM)	N MTW (Mean ± SEM)	τ (s) MTW (Mean ± SEM)	F^0 (pN) AFM (Mean ± SD)	Initiation force (pN) AFM (Mean ± SD)	F (pN) MTW (Mean ± SEM)	A (μm) MTW (Mean ± SEM)
HB (control) $n = 113$ tethers, 16 cells	$(1.2 \pm 0.5) \times 10^{-2}$	1.6 ± 0.2	$(4.5 \pm 1.0) \times 10^{-2}$	16 ± 2	0.28 ± 0.05	19.0 ± 2	522 ± 303	2.1 ± 0.3	59.2 ± 3.5
HB (latrunculin A) $n = 106$ tethers, 16 cells	$(1.1 \pm 0.2) \times 10^{-2}$	0.8 ± 0.2[a]	$(8.4 \pm 1.3) \times 10^{-2}$[a]	14 ± 2	0.12 ± 0.02[a]	13.4 ± 2.5[a]	120 ± 56[a]	2.9 ± 0.4	30.5 ± 8.3[a]
CHO $n = 85$ tethers, 7 cells	$(7.9 \pm 1.3) \times 10^{-2}$[a]	2.1 ± 0.2[a]	$(4.9 \pm 0.3) \times 10^{-1}$[a]	26 ± 5[a]	0.15 ± 0.02[a]	23.2 ± 2[a]	586 ± 218	7.7 ± 1.9[a]	16.3 ± 4.2[a]

[a] Significantly different from HB control ($p < 0.01$).
N = the number of tethers at the beginning of the pulling; F = average force/tether at the beginning of the pulling; A = terminal tether length before the first rupture (fitting parameter).

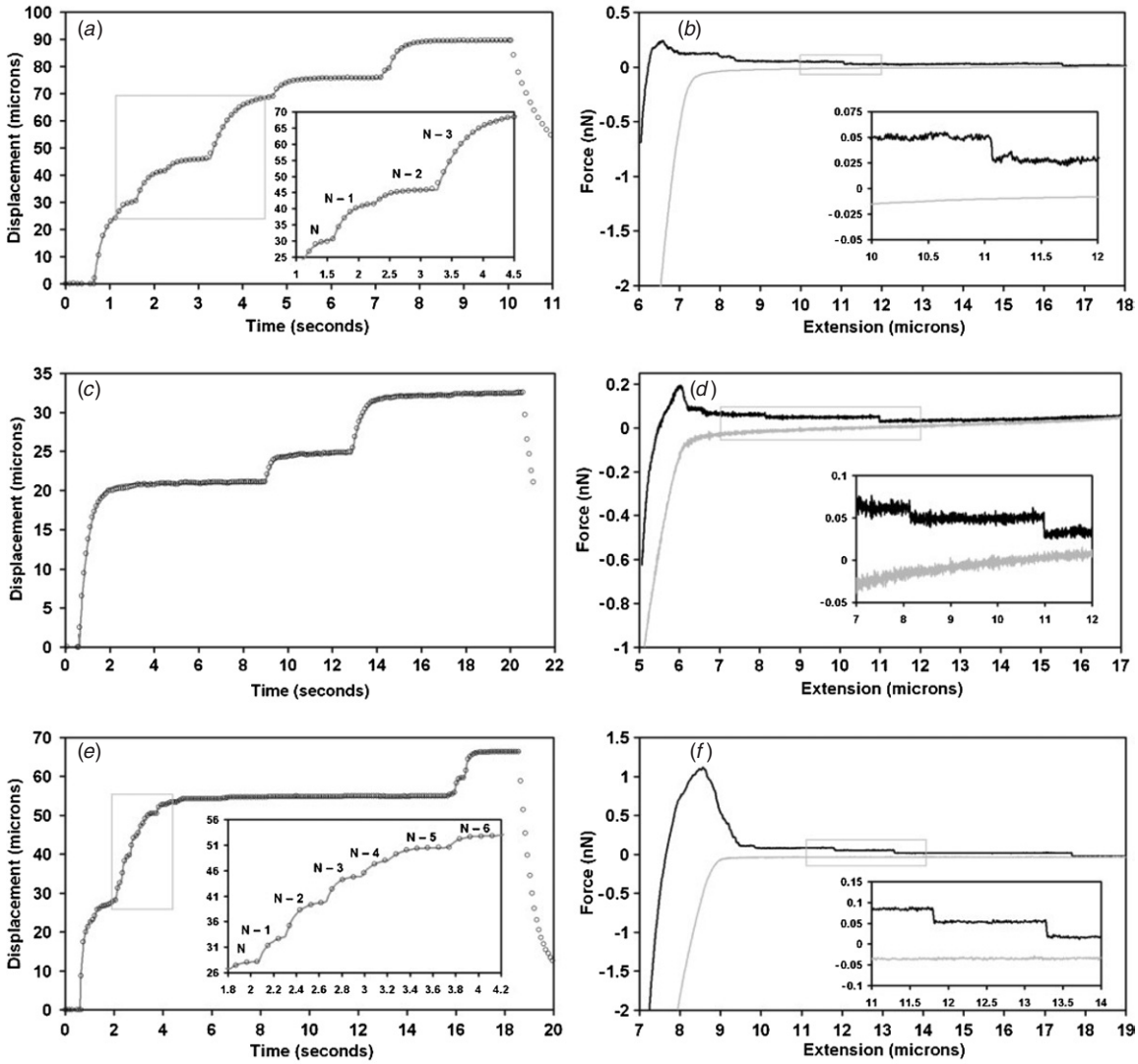

Figure 3. Typical bead trajectories in tether pulling experiments performed with MTW (left panels) and AFM (right panels) in HB cells (*a*), (*b*), HB cells treated with 1 μM latrunculin A (*c*), (*d*) and CHO cells (*e*), (*f*). In MTW pullings, '0' on the vertical axis corresponds to the position of the bead before the application of the force pulse. The open circles represent data, the lines over data points are the result of modeling (discussed later in the text, where the meaning of the labels N, $N-1$, etc, is also given). Note that turning off the magnetic force results in strongly elastic contraction and return of the bead toward its original location. In AFM pullings, the gray and black curves respectively represent the approach and retraction of the cantilever (at 3 μm s^{-1}), respectively to and from the cell. Since distance is measured from the coverslip holding the cells (and not from the cell surface), the true length of a tether is smaller than that shown at its rupture. Insets are enlargements of the boxed areas. Comparison of these recordings with the SEM images in figure 2 reveals that the former contain typically fewer and shorter tethers. This is not surprising in light of the difficulties arising from the visualization of nanotubes with electron microscopy as described in the materials and methods. Bombardment with electrons and dehydration destroyed many of these delicate structures. Furthermore, tethers for SEM were pulled under weaker forces.

$\mu = 2\pi\eta_s$ (the values for F^0 and μ are listed in table 1). (Effective surface viscosity means that in general η_s contains contributions associated with the intrinsic material properties of the lipid bilayer, the interbilayer slip and the membrane's association with the underlying cytoskeleton, as discussed in detail in [50].)

3.6. Effect of cytoskeleton disruption

To test how MTW and AFM tethers couple to the cytoskeleton, the above-described experiments were repeated with latrunculin A treated HB cells. In addition to the viscoelastic parameters, in the case of MTW tethers, comparison between treated and untreated cells included also the length at which the tethers equilibrated before the first rupture and the average force exerted on each of the initial N tethers, F/N. Even though this force is an independent parameter in MTW experiments, its value provides information on the range of forces under which a MTW tether can be pulled. In the case of AFM tethers the comparison involved also $F(v)$, F_0 (see figure 6), and the amplitude of the initiation force (the peak in the AFM plots in figure 3). For MTW tethers we found that latrunculin A treatment did not affect either μ or the force per tether, but

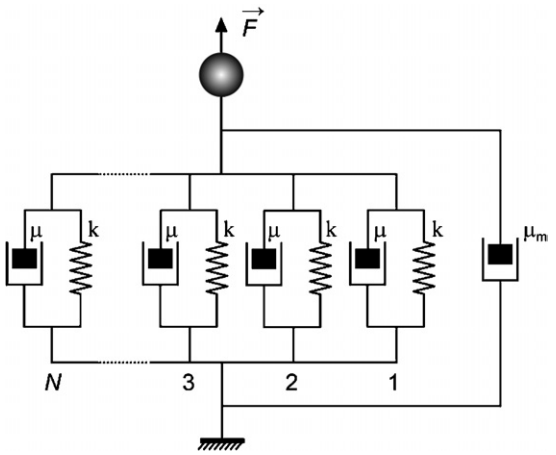

Figure 4. Voight model for multiple tether formation. Each Voight body (a dashpot with friction constant μ and spring with spring constant k) represents one of the N tethers. Tethers are assumed to be identical, non-interacting and detach one by one during the pulling experiment under the constant force F. μ_m represents the friction coefficient between the magnetic bead and the culture medium.

resulted in the decrease of tether length and increase in k (see table 1). For AFM tethers, the treatment decreased $F(v)$ (the result for 3 μm s^{-1} retraction speed was reported in [40]), F_0, μ and the initiation force (see table 1).

4. Conclusions and outlook

Membrane tethers are ubiquitous structures that have been shown to participate in numerous cell functions. When they form under physiological conditions, they do so 'en masse' [1, 2, 5, 6]. The objective of the present work was to unequivocally demonstrate that the eukaryotic cell membrane can simultaneously sprout multiple tethers, investigate the mechanisms of multiple tether formation and explore the possibility for the existence of tethers of different origin.

To accomplish this, we primarily employed MTW. The use of the MTW in combination with optical and scanning electron microscopy allowed the direct visual observation of multiple tethers (figure 2). SEM also provided high magnification images of the cell surface, with suggestive evidence for the possibility of extracting tethers with different properties (figure 1). To make quantitative comparison between tethers formed by distinct methods we also used AFM (figure 6). Nanotubes were formed through nonspecific contact, using magnetic beads and cantilevers with generic surface properties. MTW tethers are pulled with constant force and their multiplicity is detected through their ruptures producing abrupt changes in the bead displacement–time profiles (figures 3, 5). AFM tethers are pulled with constant velocity and their ruptures generate sharp drops in the force–cantilever elongation profiles (figure 3 see also [40]).

A simple model of viscoelasticity, set up for the interpretation of the MTW data (figure 4) allowed determination of the total number, N, of tethers in individual pulling experiments (figure 5). The values of N, obtained from the model varied between 12 and 48, and 9 and 34,

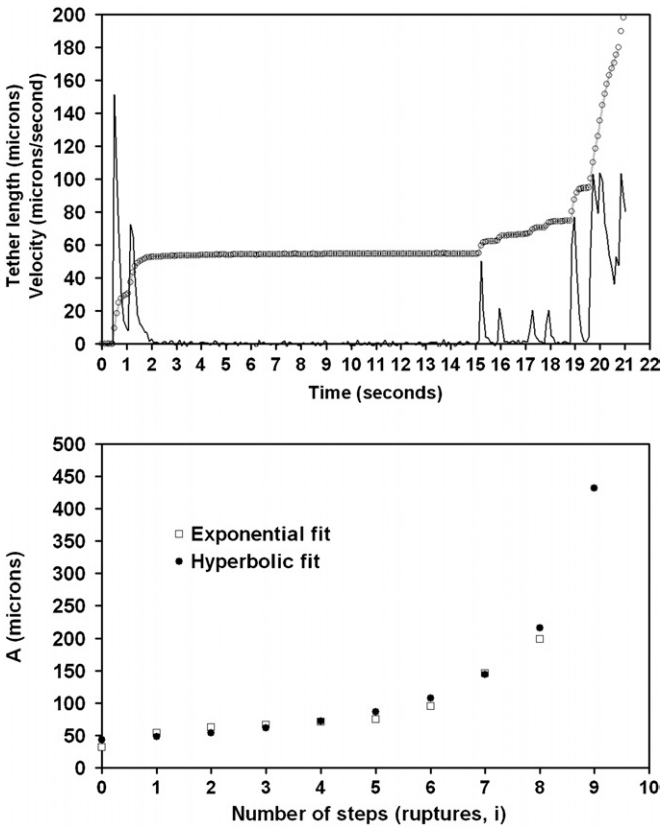

Figure 5. Estimating the total number of tethers in an MTW experiment. Top. Typical bead trajectory (open circles) fit with the Voight model for multiple tether formation (line over data points). The spiky curve represents the bead's instantaneous velocity. The events shown are quite heterogeneous, with short initial tethers followed by a long stable one and with renewed more frequent ruptures. Even though the variation of bead velocity at ruptures in this curve (generated with a HB cell with a magnetic force of 15 pN) is typical, the long plateau is not. More typically, longer and shorter segments occur in random sequence as reflection of the random character of tether lifetime. It is used here because all rupture events, in particular the last one, can be identified and thus the analysis for the total number of tethers conveniently carried out (see below). Bottom. The parameters A_i ($i = 0, 1, \ldots, N-1$) obtained from the exponential fit to data (open squares) and deduced from the hyperbolic function $A(x) = F/[k(N-x)]$ as a result of modeling (filled circles, see the text), for the trajectory shown on the top. The hyperbolic fit provides the total number of extracted tethers, $N = 10$ (in good agreement with what can be counted along the trajectory) and the ratio F/k, and thus k.

respectively for the CHO and HB cells. (The largest number of experimentally clearly discernable rupture events was 22 for CHO and 12 for HB cells.) The number of MTW tethers in each individual experiment is consistent with the relatively large diameter of the magnetic beads (5 μm), which can easily accommodate binding sites for several tethers. (Note that the diameter of the magnetic bead is comparable to the size of the inset in figure 1.) The plateau values of the bead displacements seen in figure 3 prior to ruptures correspond to the maximum length of the 'tether-springs' under the applied force. As more tethers rupture and the force per tether increases, so does the terminal length of the remaining ones (i.e. A_i increases with i).

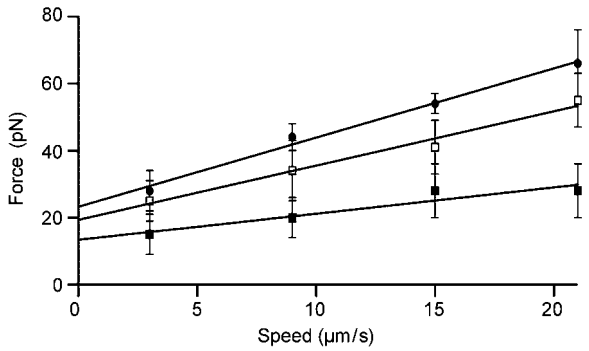

Figure 6. Tether force versus tether growth velocity (i.e. AFM cantilever retraction speed). Data are shown for four cantilever retraction speeds: 3, 9, 15 and 21 μm s^{-1} (results for 3 μm s^{-1} are from [40], figure 3). Circles and squares are the data, respectively for CHO and HB cells (control—open squares; latrunculin A treated—filled squares). Lines are linear fits to the data ($R^2 = 0.99, 0.96$, respectively for CHO and HB cells).

Tether formation requires initiation, which takes place quite differently in experiments performed with MTW and AFM. In the MTW experiments contact between the force transducer and the membrane material was established by the gravitational fall of a magnetic bead (5 μm diameter, 1.5 g cm^{-3} density) through tissue culture medium, producing an overall force on the cell of <1 pN. In the AFM experiments contact was detected through the deflection of the cantilever. Due to the force resolution, in the AFM technique the contact force is minimum 10–20 pN. (In reality the contact force often was several nanonewtons, to assure the extraction of multiple tethers; see figure 3.)

As the results listed in table 1 indicate tethers produced with MTW and AFM have quite different physical properties. Pulling forces for individual AFM tethers, originating from cells with intact cytoskeleton, are 20–30 pN even at the lowest retraction speed (figure 6 and [40]), whereas for MTW tethers they can be as low as 1.5 pN (obtained from the ratio of the known applied force and the number of clearly discernable rupture events, figure 5). The characteristic friction constants μ_{CHO} and μ_{HB} are significantly smaller for the MTW tethers than for the AFM tethers. Their values are similar to data reported in the literature on the effective membrane surface viscosity, η_s ($\mu = 2\pi\eta_s$) for bilayer vesicles [51, 52] in the case of MTW tethers and for cellular membranes [31, 39, 53] in the case of AFM tethers.

The values of the friction constants for the MTW tethers were deduced from the Voight parameters regressed from the experiments and thus are strongly model dependent. In the case of AFM tethers these values are based on Stokes' law, thus, in principle, are not model dependent. Although it is tempting to interpret the differences in the friction constants as a signature of distinct types of tethers, *a priori* it cannot be excluded that they are due solely to the different methods used. We therefore sought for a model independent way to determine the μ values for the MTW tethers. We considered the very initial slope in the MTW displacement–time curves (figure 3), before any rupture. For this early $t/\tau_0 \ll 1$ situation the exponential fit to the curves provides the expression for the bead velocity v in terms of the fitting parameters A and τ_0. Since the early phase of tether elongation is viscosity-dominated, we also have $v = F/(N\mu + \mu_m)$, where F is the constant force provided by the tweezers and N is the total number of tethers pulled. We employed these two expressions for the speed to obtain a value for $N\mu$ using a number of displacement–time curves. In each case $N\mu$ ($N > 1$) was found to be still smaller than the results obtained for μ using the AFM data. (For the curve in figure 5, where $N = 10$, this method leads to $\mu = 0.01$ pNs μm^{-1}, which, within the accuracy of our measurements agrees with the model dependent value of the friction constant listed in table 1.)

The results in figures 3 and 5 indicate that tethers produced with MTW are typically considerably longer (~35–90 μm in figure 3, ~160 μm in figure 5) than those extracted with AFM (<15 μm, see also the legend to figure 3). This could be indicative of the MTW and AFM tethers having separate membrane reservoirs.

The above findings suggest that MTW and AFM tethers represent distinct membrane structures. This is substantiated by the analysis of the mechanisms by which these structures might originate. Producing MTW tethers does not require any detectable initiation force, no matter how many are produced, an indication that such tethers originate from pre-existing structures (in which the plasma membrane is already highly curved), possibly microvilli (figure 1), which the magnetic bead contacts during its gravitational descent (and with which it establishes practically force-free contact). AFM tethers appear only after a substantial initial force has been overcome (peak force, in figure 3), and their number depends on the strength and duration of the contact between the cantilever and the cell (results not shown). The force resolution of AFM (~10–20 pN) makes it impossible to observe structures that can be pulled with 1.5 pN, as the case with MTW tethers.

It is unlikely that the AFM-generated structures could ever be observed with our constant force MTW. Results in the right panels of figure 3 suggest that even if contact between the cantilever and the cell gives rise to numerous tethers most of them detach before the first well-developed plateau appears (at which point there remain four in the case shown in panels (*b*) and (*f*) in figure 3, and three in panel (*d*)). If these tethers were to be extracted with the MTW at constant pulling forces into the nanonewtons (as in the case of AFM), they would likely all vanish shortly after they appear, because, unlike in the AFM case, once the initiation force is applied, it would remain constant for the rest of the pulling. Thus the force exerted per tether would never decrease; it would increase as the tethers rupture. A further implication of these findings is that AFM tethers are extracted *de novo* from the cell's membrane reservoir, or from structures that require overcoming finite initiation force. The different association of the cytoskeleton with these structures may explain the dissimilar physical properties of the two types of tethers.

A further indication that MTW and AFM tethers are indeed distinct in their origin and structure is provided by their response to F actin disruption. Latrunculin A treatment did not significantly change the friction constant associated with MTW tethers. These results are similar to those reported

in [29], where structures similar to our MTW tethers were investigated. Authors of that work used optical tweezers to extract single tethers from terminally differentiated fibroblasts and mesenchymal stem cells (MSC). Although the pulling method resembled our AFM experiments (constant velocity pulling while monitoring the tether force), the experimental conditions were closer to those in our MTW measurements: beads were attached to cells by gravitational fall. The outcome of these experiments has striking similarities to our MTW experiments. It was found that single membrane tethers could be extracted with very low forces, similar to the ones exerted in our MTW experiments (∼3 pN, much smaller than in our AFM experiments) without any initiation force. Cytoskeleton disruption had no effect on MSCs. In particular the tether force and tether length did not change, whereas these quantities decreased in the case of fibroblasts. Even though the tether friction coefficient was unaffected by latrunculin A in our MTW experiments, the resulting tethers had shorter length under the same force (as assessed by their equilibrium length before the first rupture, table 1) and were stiffer (k increased, table 1). This suggests that latrunculin A treatment results in the decrease in the MTW membrane reservoir. A possible reason for this is the known property of this drug to modulate the cell's osmotic homeostasis by activating the Na channels in the plasma membrane [55, 56], which induces cell swelling thus decreasing the membrane reservoir. It is worth noting that stem and tumor cells do have common properties: neither cell type has the features of terminally differentiated cells. Tumor cells start out as differentiated cells but, due to their rapid proliferation, gradually lose their original lineage specification. The properties of AFM tethers (see table 1) are strongly affected by cytoskeleton disruption: each parameter significantly decreased upon latrunculin A treatment, in particular the friction coefficient. These results imply that the membrane reservoir that gives rise to MTW tethers adheres much less to the cytoskeleton than the one providing membrane material for the AFM tethers.

The observed differences between the MTW and AFM tethers could in principle have their origin in the differences in the attachment of the bead and the cantilever to the cell, contact duration and geometry and experimental conditions. It is true that the surfaces of the two force transducers are quite different: polystyrene coating in one case and silicone nitrite in the other. However, the nature of contact primarily affects the lifetime of the attachment and not the material properties of the tethers [31]. Contact geometry (e.g. bead diameter [29]) and duration prior to pulling [40] influence the number of nanotubes, but not other aspects of tether extraction. Finally, it is precisely due to differing experimental conditions that the two methods can detect membrane tethers of distinct origin.

We believe, our results have important biological implications. They indicate that a true cell membrane is capable of sprouting multiple nonspecific tethers as soon as it can physically attach to a substrate (i.e. the surface of the magnetic bead or the cantilever). At the same time, specific receptor–ligand bonds also might give rise to such structures. A particularly instructive example is provided by Puech and coworkers [57]. These authors studied the modulation of specific adhesion between zebrafish mesendodermal cells and fibronectin surfaces, through the *wnt11* gene product, using similar AFM force spectroscopy as described in [40] and here. The shape of force–elongation curves (figure 3 in [57]) recorded by these authors, for all practical purposes is identical to the one shown here in figure 3 (or in figure 3 in [40]), both exhibiting a sequence of force drops of similar magnitude corresponding to rupture or detachment events. Without further study (e.g. blocking specific integrin–fibronectin bonds or mutating the *wnt11* gene) it is impossible to establish which rupture event corresponds to the breakage of a specific bond or the detachment of a tether. Our work suggests, along with others [58], that nonspecific interactions may be important under physiological conditions.

In conclusion, the application of magnetic tweezers and scanning electron microscopy allowed gaining further insight into the mechanisms of multiple membrane nanotube formation. When compared with tether extraction through atomic force microscopy, our findings suggest that the physical properties of these processes (and thus most probably their biological functions) depend on local cell surface characteristics and on how they originate. Our findings also imply that as long as living cells can attach to substrates (under physiological conditions these could be other cells or extracellular structures) distinguishing between tethers formed through specific and nonspecific interactions is highly nontrivial if at all possible.

Acknowledgments

The authors would like to thank Imre Derényi, Evan Evans, Michael Sheetz and Yuri Korchev for useful discussions. This study was partially supported by grants from NSF and NASA (to GF) and NSERC (MG).

Glossary

Magnetic tweezers. Device capable of exerting localized forces on biological materials through magnetic particles (beads) attached to the structure of interest.

Atomic force microscope. A device that can be used to investigate the strength of adhesive molecular interactions established between the structure of interest (e.g. tether) and an elastic cantilever, through the bending of the latter.

Membrane tether. Nanotubular structure that can be pulled out of phospholipid bilayers as a result of applying localized forces.

Relaxation time. A material parameter: the time scale on which a given material recovers from a certain type of perturbation.

References

[1] Schmidtke D W and Diamond S L 2000 Direct observation of membrane tethers formed during neutrophil attachment to platelets or P-selectin under physiological flow *J. Cell Biol.* **149** 719–30

[2] Ramachandran V, Williams M, Yago T, Schmidtke D W and McEver R P 2004 Dynamic alterations of membrane tethers stabilize leukocyte rolling on P-selectin *Proc. Natl Acad. Sci. USA* **101** 13519–24

[3] Alon R, Chen S, Fuhlbrigge R, Puri K D and Springer T A 1998 The kinetics and shear threshold of transient and rolling interactions of L-selectin with its ligand on leukocytes *Proc. Natl Acad. Sci. USA* **95** 11631–6

[4] McCarty O J, Mousa S A, Bray P F and Konstantopoulos K 2000 Immobilized platelets support human colon carcinoma cell tethering, rolling, and firm adhesion under dynamic flow conditions *Blood* **96** 1789–97

[5] Rustom A, Saffrich R, Markovic I, Walther P and Gerdes H H 2004 Nanotubular highways for intercellular organelle transport *Science* **303** 1007–10

[6] Vidulescu C, Clejan S and O'Connor C K 2004 Vesicle traffic through intercellular bridges in DU 145 human prostate cancer cells *J. Cell Mol. Med.* **8** 388–96

[7] Polishchuk E V, Di Pentima A, Luini A and Polishchuk R S 2003 Mechanism of constitutive export from the golgi: bulk flow via the formation, protrusion, and en bloc cleavage of large trans-golgi network tubular domains *Mol. Biol. Cell* **14** 4470–85

[8] White J *et al* 1999 Rab6 coordinates a novel Golgi to ER retrograde transport pathway in live cells *J. Cell Biol.* **147** 743–60

[9] Iglic A, Hägerstrand H, Bobrowska-Hägerstrand M, Arrigler V and Kralj-Iglic V 2003 Possible role of phospholipid nanotubes in directed transport of membrane vesicles *Phys. Lett.* A **310** 493–7

[10] Upadhyaya A and Sheetz M P 2004 Tension in tubulovesicular networks of Golgi and endoplasmic reticulum membranes *Biophys. J.* **86** 2923–8

[11] Giuffre L, Cordey A S, Monai N, Tardy Y, Schapira M and Spertini O 1997 Monocyte adhesion to activated aortic endothelium: role of L-selectin and heparan sulfate proteoglycans *J. Cell Biol.* **136** 945–56

[12] Sheetz M P 1995 Cellular plasma membrane domains *Mol. Membr. Biol.* **12** 89–91

[13] Roux A, Cappello G, Cartaud J, Prost J, Goud B and Bassereau P 2002 A minimal system allowing tubulation with molecular motors pulling on giant liposomes *Proc. Natl Acad. Sci. USA* **99** 5394–9

[14] Leduc C, Campas O, Zeldovich K B, Roux A, Jolimaitre P, Bourel-Bonnet L, Goud B, Joanny J-F, Bassereau P and Prost J 2004 Cooperative extraction of membrane nanotubes by molecular motors *Proc. Natl Acad. Sci. USA* **101** 17096–101

[15] Koster G, VanDuijn M, Hofs B and Dogterom M 2003 Membrane tube formation from giant vesicles by dynamic association of motor proteins *Proc. Natl Acad. Sci. USA* **100** 15583–8

[16] Waugh R E and Hochmuth R M 1987 Mechanical equilibrium of thick, hollow, liquid membrane cylinders *Biophys. J.* **52** 391–400

[17] Bo L and Waugh R E 1989 Determination of bilayer membrane bending stiffness by tether formation from giant, thin-walled vesicles *Biophys. J.* **55** 509–17

[18] Waugh R E, Song J, Svetina S and Zeks B 1992 Local and nonlocal curvature elasticity in bilayer membranes by tether formation from lecithin vesicles *Biophys. J.* **61** 974–82

[19] Derenyi I, Julicher F and Prost J 2002 Formation and interaction of membrane tubes *Phys. Rev. Lett.* **88** 238101

[20] Cuvelier D, Derenyi I, Bassereau P and Nassoy P 2005 Coalescence of membrane tethers: experiments, theory, and applications *Biophys. J.* **88** 2714–26

[21] Koster G, Cacciuto A, Derenyi I, Frenkel D and Dogterom M 2005 Force barriers for membrane tube formation *Phys. Rev. Lett.* **94** 068101

[22] Hochmuth R M and Marcus W D 2002 Membrane tethers formed from blood cells with available area and determination of their adhesion energy *Biophys. J.* **82** 2964–9

[23] Sheetz M P 2001 Cell control by membrane-cytoskeleton adhesion *Nat. Rev. Mol. Cell Biol.* **2** 392–6

[24] Dai J and Sheetz M P 1999 Membrane tether formation from blebbing cells *Biophys. J.* **77** 3363–70

[25] Shao J-Y, Ting-Beall H P and Hoshmuth R M 1998 Static and dynamic lengths of neutrophil microvilli *Proc. Natl Acad. Sci. USA* **95** 6707–802

[26] Dai J and Sheetz M P 1995 Mechanical properties of neuronal growth cone membranes studied by tether formation with laser optical tweezers *Biophys. J.* **68** 988–96

[27] Raucher D, Stauffer T, Chen W, Shen K, Guo S, York J D, Sheetz M P and Meyer T 2000 Phosphatidylinositol 4,5-bisphosphate functions as a second messenger that regulates cytoskeleton-plasma membrane adhesion *Cell* **100** 221–8

[28] Inaba T, Ishijima A, Honda M, Nomura F, Takiguchi K and Hotani H 2005 Formation and maintenance of tubular membrane projections require mechanical force, but their elongation and shortening do not require additional force *J. Mol. Biol.* **348** 325–33

[29] Titushkin I and Cho M 2006 Distinct membrane mechanical properties of human mesenchymal stem cells determined using laser optical tweezers *Biophys. J.* **90** 2582–91

[30] Heinrich V and Waugh R E 1996 A piconewton force transducer and its application to measurement of the bending stiffness of phospholipid membranes *Ann. Biomed. Eng.* **24** 595–605

[31] Girdhar G and Shao J Y 2004 Membrane tether extraction from human umbilical vein endothelial cells and its implication in leukocyte rolling *Biophys. J.* **87** 3561–8

[32] Shao J Y and Hochmuth R M 1996 Micropipette suction for measuring piconewton forces of adhesion and tether formation from neutrophil membranes *Biophys. J.* **71** 2892–901

[33] Shao J Y and Xu J 2002 A modified micropipette aspiration technique and its application to tether formation from human neutrophils *J. Biomech. Eng.* **124** 388–96

[34] Hochmuth R M, Wiles H C, Evans E and McCown J T 1982 Extensional flow of erythrocyte membrane from cell body to elastic tether *Biophys. J.* **39** 83–9

[35] Zhelev D V and Hochmuth R M 1995 Mechanically stimulated cytoskeleton rearrangement and cortical contraction in human neutrophils *Biophys. J.* **68** 2004–14

[36] Dai J, Sheetz M P, Wan X and Morris C E 1998 Membrane tension in swelling and shrinking molluscan neurons *J. Neurosci.* **18** 6681–92

[37] Raucher D and Sheetz M P 1999 Characteristics of a membrane reservoir buffering membrane tension *Biophys. J.* **77** 1992–2002

[38] Raucher D and Sheetz M P 2001 Phospholipase C activation by anesthetics decreases membrane-cytoskeleton adhesion *J. Cell Sci.* **114** 3759–66

[39] Xu G and Shao J Y 2005 Double tether extraction from human neutrophils and its comparison with CD4+ T-lymphocytes *Biophys. J.* **88** 661–9

[40] Sun M, Graham J S, Hegedüs B, Marga F, Zhang Y, Forgacs G and Grandbois M 2005 Multiple membrane tethers probed by atomic force microscopy *Biophys. J.* **89** 1–10

[41] Clausen-Schaumann H, Seitz M, Krautbauer R and Gaub H E 2000 Force spectroscopy with single bio-molecules *Curr. Opin. Chem. Biol.* **4** 524–30

[42] Zlatanova J, Lindsay S M and Leuba S H 2000 Single molecule force spectroscopy in biology using the atomic force microscope *Prog. Biophys. Mol. Biol.* **74** 37–61

[43] Hosu B G, Jakab K, Banki P, Toth F I and Forgacs G 2003 Magnetic tweezers for intracellular applications *Rev. Sci. Instrum.* **74** 4158–63
[44] Hegedus B, Czirok A, Fazekas I, Abel T B, Madarasz E and Vicsek T 2000 Locomotion and proliferation of glioblastoma cells in vitro: statistical evaluation of videomicroscopic observations *J. Neurosurg.* **92** 428–34
[45] Coue M, Brenner S L, Spector I and Korn E D 1987 Inhibition of actin polymerization by latrunculin A *FEBS Lett.* **213** 316–8
[46] Spector I, Shochet N R, Blasberger D and Kashman Y 1989 Latrunculins—novel marine macrolides that disrupt microfilament organization and affect cell growth. I. Comparison with cytochalasin D *Cell Motil. Cytoskel.* **13** 127–44
[47] Yarmola E G, Somasundaram T, Boring T A, Spector I and Bubb M R 2000 Actin-latrunculin A structure and function *J. Biol. Chem.* **275** 28120–7
[48] Fung Y C 1993 *Biomechanics: Mechanical Properties of Living Tissues* (New York: Springer)
[49] Heinrich V, Leung A and Evans E 2005 Nano- to microscale dynamics of P-selectin detachment from leukocyte interfaces: II. Tether flow terminated by P-Selectin dissociation from PSGL-1 *Biophys. J.* **88** 2299–308
[50] Hochmuth F M, Shao J Y, Dai J and Sheetz M P 1996 Deformation and flow of membrane into tethers extracted from neuronal growth cones *Biophys. J.* **70** 358–69
[51] Waugh R E 1982 Surface viscosity measurements from large bilayer vesicle tether formation: II. Experiments *Biophys. J.* **38** 29–37
[52] Evans E and Yeung A 1994 Hidden dynamics in rapid changes of bilayer shape *Chem. Phys. Lipids.* **73** 39–56
[53] Li Z, Anvari B, Takashima M, Brecht P, Torres J H and Brownell W E 2002 Membrane tether formation from outer hair cells with optical tweezers *Biophys. J.* **82** 1386–95
[54] Edmondson K E, Denney W S and Diamond S L 2005 Neutrophil-bead collision assay: pharmacologically-induced changes in membrane mechanics regulate the PSGL-1/P-selectin adhesion lifetime *Biophys. J.* **89** 3603–14
[55] Kerrigan M J, Hook C S, Qusous A and Hall A C 2006 Regulatory volume increase (RVI) by in situ and isolated bovine articular chondrocytes *J. Cell Physiol.* **209** 481–92
[56] Bustamante M, Roger F, Bochaton-Piallat M L, Gabbiani G, Martin P Y and Feraille E 2003 Regulatory volume increase is associated with p38 kinase-dependent actin cytoskeleton remodeling in rat kidney MTAL *Am. J. Physiol. Renal Physiol.* F336–47
[57] Puech P-H, Taubenberger A, Ulrich F, Krieg M, Muller D J and Heisenberg C-P 2005 Measuring cell adhesion forces of primary gastrulating cells from zebrafish using atomic force microscopy *J. Cell Sci.* **118** 4199–206
[58] Kalodimos C G, Biris N, Bonvin A M, Levandoski M M, Guennuegues M, Boelens R and Kaptein R 2004 Structure and flexibility adaptation in nonspecific and specific protein-DNA complexes *Science* **305** 386–9